SF2A 2010
S. Boissier, M. Heydari-Malayeri, R. Samadi and D. Valls-Gabaud (eds)

GALAXY STELLAR MASS ASSEMBLY BETWEEN $0.2 < Z < 2$ FROM THE S-COSMOS SURVEY

O. Ilbert[1], M. Salvato[2], E. Le Floc'h[3], H. Aussel[4], P. Capak[5], H.J. McCracken[6], B. Mobasher[7], J. Kartaltepe[8], N. Scoville[2], D.B. Sanders[8] and the COSMOS team

Abstract. We follow the galaxy stellar mass assembly by morphological and spectral type in the COSMOS 2-deg^2 field. We derive the stellar mass functions from $z = 2$ to $z = 0.2$ using 196,000 galaxies selected at $F_{3.6\mu m} > 1\mu Jy$ with accurate photometric redshifts ($\sigma_{(z_{phot}-z_{spec})/(1+z_{spec})} = 0.008$ at $i^+ < 22.5$). First, we find that the massive galaxies with the highest SSFR end their star formation phase first, following a downsizing pattern. Secondly, the mass function of the overall star-forming population doesn't evolve significantly at $z < 1$. Then, we find that the density of massive quiescent galaxies increases rapidly between $z = 2$ and $z = 1$ and this evolution slows down significantly after $z < 1$. The density of quiescent galaxies increases at low/intermediate masses. Adding the morphological information, we find that elliptical galaxies represents 80-90% of the massive quiescent galaxies at $z < 0.8$. Still, a significant fraction of quiescent galaxies present a Spi/Irr morphology at low mass (40-60% at $log(\mathcal{M}) \sim 9.5$). We find a population of blue elliptical galaxies which are mostly low mass galaxies at $z < 1$. This analysis is detailed in Ilbert et al. (2010).

Keywords: galaxies: luminosity function and mass function, galaxies: evolution, galaxies: formation

1 Introduction

A clear and comprehensive picture describing the physical processes which regulate stellar mass growth in galaxies is still missing in our understanding of galaxy evolution. Indeed, the stellar mass growth is regulated by a complex interplay between the radiative cooling of the gas (e.g. White 1978), cold accretion (e.g. Kereš et al. 2005), the spatial redistribution of the gas along the hierarchical growth of dark matter halos (e.g. Springel et al. 2006) and the feedback from supernovae and Active Galaxy Nuclei (e.g. Benson et al. 2003, Croton et al. 2006). Merging between galaxies is another central mechanism in stellar mass assembly. Indeed, mergers are expected to create new high-mass galaxies and to modify deeply galaxy properties (morphology and spectral type). The stellar mass function (MF) characterizes how star formation activity build the stellar mass and how mergers redistribute this stellar mass depending on the galaxy type.

We follow the evolution of the galaxy stellar mass function using the COSMOS survey (Scoville et al. 2007). The extensive multi-λ coverage of COSMOS provides accurate photometric redshifts (Ilbert et al. 2009). Combined with deep *Spitzer*/IRAC and NIR data (Sanders et al. 2007, McCracken et al. 2009), we estimate accurate stellar masses out to $z \sim 2$. Following the stellar mass assembly of a given galaxy population requires that the sample be split into well characterized galaxy types. We took special care to characterize the galaxy populations, using the specific star formation rate (SSFR) derived from SED fitting and a morphological classification carried out based on the HST/ACS images.

[1] Laboratoire d'Astrophysique de Marseille, Université de Provence, CNRS, BP 8, Traverse du Siphon, 13376 Marseille Cedex 12, France
[2] California Institute of Technology, MC 105-24, 1200 East California Boulevard, Pasadena, CA 91125
[3] CEA/DSM-CNRS, CEA, Saclay
[4] AIM Unité Mixte de Recherche CEA CNRS Université Paris VII UMR n158
[5] Spitzer Science Center, California Institute of Technology, Pasadena, CA 91125
[6] Institut d'Astrophysique de Paris, UMR7095 CNRS, Université Pierre et Marie Curie, 98 bis Boulevard Arago, 75014 Paris, France
[7] Department of Physics and Astronomy, University of California, Riverside, CA, 92521, USA
[8] Institute for Astronomy, 2680 Woodlawn Dr., University of Hawaii, Honolulu, Hawaii, 96822

2 Data

This analysis is based on a mass selected sample as generated from the $3.6\mu m$ IRAC catalogue of the S-COSMOS survey (Sanders et al. 2007). The IRAC data were taken during the Spitzer Cycle 2 S-COSMOS survey, which used 166 hrs to map the full 2-deg^2 COSMOS field. The source catalogue is extracted using the SExtractor software (Bertin & Arnouts, 1996). The source detection is performed at $3.6\mu m$. The IRAC catalogue is 90% complete at 5 μJy and 50% complete at 1 μJy.

We derive photometric redshifts using the *Le Phare*[1] code (Arnouts & Ilbert) with a χ^2 template-fitting method. The photo-z are computed using 31 bands (new H band data in comparison to Ilbert et al. 2009). The comparison between the photometric and spectroscopic redshifts from the zCOSMOS survey (Lilly et al. 2007) shows that the fraction of outliers is less than 1% and the accuracy is as good as $\sigma_{(z_{phot}-z_{spec})/(1+z_{spec})} = 0.008$ at $i^+_{AB} < 22.5$.

We cross-match the $3.6\mu m$ and photo-z catalogues by taking the closest counterpart within a radius of $1''$. We identify 2714 IRAC sources which are clearly non-detected in optical and are detected in the K-band selected catalogue. We measure a photo-z for these sources using NIR and IRAC data and an upper-limit was set in i^+.

Finally, we remove all of the sources flagged as star (χ^2 criteria) or AGN (detected with XMM-COSMOS). The final sample contains 196,000 galaxies at $F_{3.6\mu m} > 1\mu Jy$ over an effective area of 1.73-deg^2.

3 Method to compute the stellar mass function

We use stellar population synthesis (SPS) models to convert luminosity into stellar mass. The SED templates are generated with the stellar population synthesis package developed by Bruzual & Charlot (2003). We assume an universal IMF from Chabrier (2003), two different metallicities and an exponentially declining star formation history $SFR \propto e^{-t/\tau}$. Dust extinction is applied to the templates using the Calzetti et al. (2000) law. The difference between the stellar masses computed with the photometric and spectroscopic redshifts has a dispersion smaller than ~ 0.03 dex ($10\times$ smaller than the expected systematic uncertainties).

We measure the stellar mass functions using the tool ALF (*Algorithm for Luminosity Function*). This tool includes the STY parametric estimator, the $1/V_{max}$, the C^+ and the Step-Wise Maximum Likelihood. The estimators included in ALF are described in detail in appendix 2 of Ilbert et al. (2005). The low mass limits considered for the MF estimates are set in order to insure a complete and unbiased stellar mass sample with accurate photo-z (less than 30% of $i^+_{AB} > 25.5$ in the lowest stellar mass bin). Finally, we performed extensive simulations in order to propagate the photo-z uncertainties into the mass function.

4 Mass function by spectral and morphological type

First, we isolate "quiescent" galaxies based on the best-fit templates ($SSFR < 10^{-11}$) . Our "quiescent" population matches well with the red clump galaxies found by Williams et al. (2008) and we separate well "quiescent" galaxies and a dust-extincted star-forming population. Fig. 1 shows the MF of the quiescent galaxies (red curves). We find that: **i)** the density of "quiescent" galaxies more massive than $log(\mathcal{M}) > 11$ increases by a factor of ~ 14 between $z = 1.5 - 2$ and $z = 0.8 - 1$; **ii)** this evolution slows down significantly after $z < 1$ and the high-mass exponential cutoff does not increase by more than 0.2 dex at $z < 1$; **iii)** the density of quiescent galaxies increases at intermediate mass between $z = 0.8 - 1$ and $z = 0.2 - 0.4$ (continuous steepening of the slope α with time).

Secondly, we add the morphological information in our classification scheme. We use the high resolution HST/ACS images (Koekemoer et al. 2007) to perform a morphological classification of our galaxy sample and we separate E/S0 and Spi/Irr galaxies. At high mass, $log(\mathcal{M}) \sim 10.5$, the fraction of quiescent galaxies with an elliptical morphology is greater than 80% at $z < 0.8$ and decreases continuously toward low masses reaching 60% (40%) at $log(\mathcal{M}) \sim 9.5$. We find a similar MF evolution for the red ellipticals as for the quiescent galaxies: the most massive red elliptical galaxies show little evolution at $z < 1$ while their density still increases at low/intermediate masses. We also find a significant population of "blue elliptical" galaxies, which could be newly formed elliptical galaxies still consuming the gas of their progenitors. The fraction of "blue ellipticals" decreases towards high mass systems. The "blue elliptical" galaxies represent $< 20\%$ of the massive elliptical galaxies (at $log(\mathcal{M}) > 11$ and $z < 1$), but their contribution reaches 40-60% at $log(\mathcal{M}) \sim 10$.

[1]www.cfht.hawaii.edu/ arnouts/LEPHARE/cfht_lephare

Finally, we divide the star-forming sample into “intermediate activity” and “high activity” galaxies, which corresponds to two classes of SSFR ($10^{-11} < SSFR < 6.3 \times 10^{-10}$ and $SSFR > 6.3 \times 10^{-10}$, respectively). The slope of the “high activity” galaxies is always the steepest (blue curve in Fig. 1). The density of “high activity” galaxies decreases with cosmic time. The decrease is stronger for high mass galaxies. We do not observe significant changes in the MF of all star-forming galaxies, i.e. the sum of the “intermediate activity” and “high activity”. The little evolution of the star-forming MF means that a fraction of star-forming galaxies is transferred to the quiescent population (as already noted by Arnouts et al. 2007 and is discussed in Peng et al. 2010, Boissier et al. 2010). It means also that the decrease with time of “high activity” galaxies is partly counter-balanced by the build up of the “intermediate activity” MF.

5 conclusion

We follow the galaxy stellar mass assembly by morphological and spectral type in the COSMOS 2-deg^2 field from $z = 2$ to $z = 0.2$.

Using a spectral classification, we find that $z \sim 1$ is an epoch of transition in the stellar mass assembly of quiescent galaxies. Their stellar mass density increases by 1.1 dex between $z = 1.5 - 2$ and $z = 0.8 - 1$, but only by 0.3 dex between $z = 0.8 - 1$ and $z \sim 0.1$. The high-mass end of the star-forming MF is shifted below the high-mass end of the quiescent MF at $z < 1$. Therefore, we interpret the slow down in the assembly of the most massive elliptical galaxies at $z < 1$ as being due to a “lack of supply” of massive star-forming galaxies available for “wet mergers” and a poor efficiency of “dry merging” (merger between quiescent galaxies) at high mass.

Then, we add the morphological information and find that 80-90% of the massive quiescent galaxies ($log(\mathcal{M}) \sim 11$) have an elliptical morphology at $z < 0.8$. Therefore, a dominant mechanism links the shutdown of star formation and the acquisition of an elliptical morphology in massive galaxies, as might be expected in galaxy merging and/or morphological quenching (Martig et al. 2009). Still, a significant fraction of quiescent galaxies present a Spi/Irr morphology at low mass (40-60% at $log(\mathcal{M}) \sim 9.5$). This significant fraction of quenched Spi/Irr leaves room for a mechanism which shuts down the star formation without transforming their morphology, such as the impact of AGN feedback on the satellite galaxies of a massive halo (e.g. Cattaneo et al. 2006).

We also split the star-forming galaxies into two SSFR classes: “intermediate activity” and “high activity” galaxies. We find that the most massive “high activity” galaxies end their high star formation rate phase first. Therefore, this redistribution of the star formation activity follows a clear “downsizing” pattern (Cowie et al. 1996) within the star-forming sample itself.

References

Arnouts, S. et al. 2007, A&A, 476, 137

Bertin, E. & Arnouts, S. 1996, A&AS, 117, 393

Boissier, S., Buat, V., Ilbert, O. 2010, A&A, in press, astro-ph/1005.5004

Bower, R.G., Benson, A.J., Malbon, R et al., 2006, MNRAS, 370, 645

Bruzual, A.G. & Charlot, S., 2003, MNRAS, 344, 1000

Calzetti, D., Armus, L., Bohlin R.C. et al., 2000, ApJ, 533, 682

Capak, P., Abraham, R.G., Ellis, R.S. et al., 2007, ApJS, 172, 284

Cattaneo, A., Dekel, A., Devriendt, J. et al., 2006, MNRAS, 370, 1651

Chabrier, G. 2003, PASP, 115, 763

Croton, D.J., Springel, V., White, S et al. 2006, MNRAS, 365, 11

Cowie, L.L., Songaila, A., Hu, E.M. & Cohen, J.G. 1996, AJ, 112, 839

Cowie, L.L. & Barger, A.J. 2008, ApJ, 697, 122

Ilbert, O., Tresse, L., Zucca, E. et al. 2005, A&A, 439, 863

Ilbert, O., Capak, P., Salvato, M. et al. 2009, A&A, 690, 1236

Ilbert, O., Salvato, M., Le Floc'h, E. et al. 2010, ApJ, 690, 1236

Kereš, D., Katz, N., Weinberg, D.H., & Davé, R. 2005, MNRAS, 363, 2

Koekemoer, A. M., Aussel, H., Calzetti, D. et al. 2007, ApJS 172, 196

Martig M., Bournaud F., Teyssier R. & Dekel A., 2009, ApJ, 707, 250

McCracken, H.J., Capak, P., Salvato, M. et al. 2009, ApJ, 708, 702

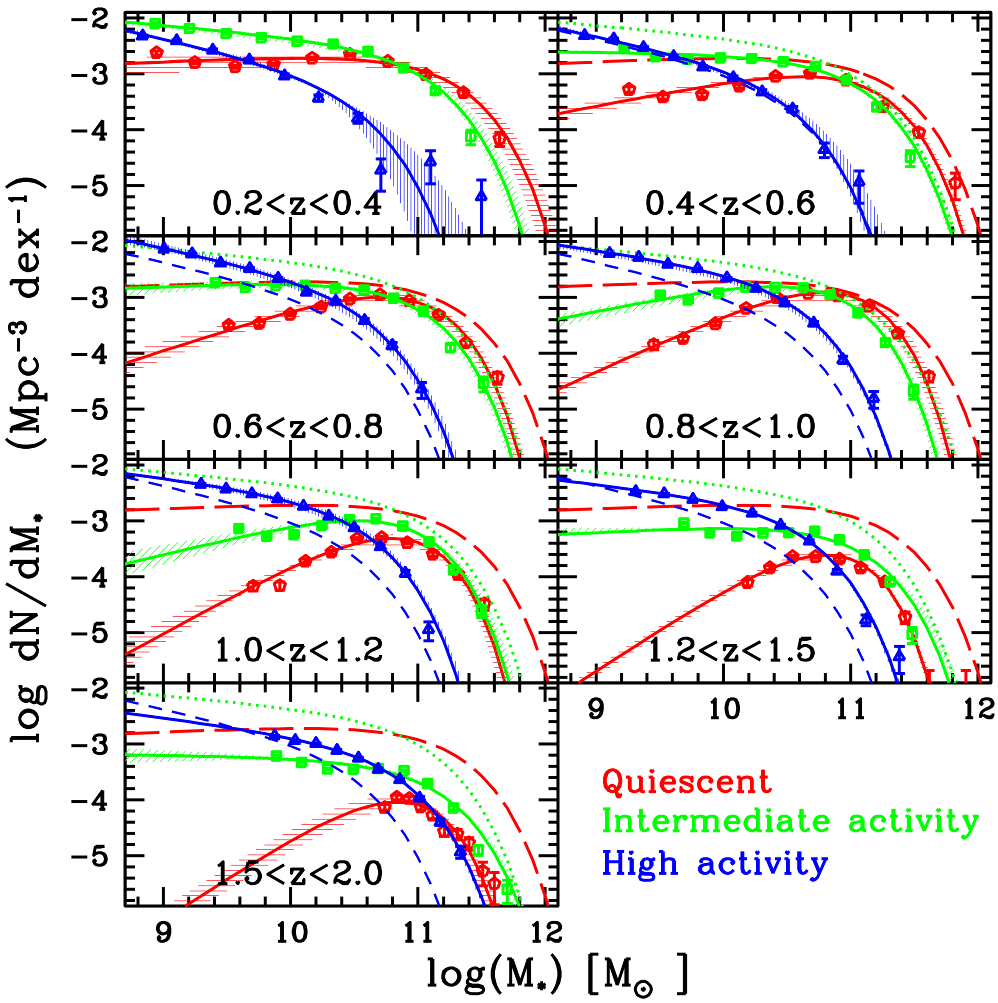

Fig. 1. MF by spectral type. The sample is split into "high activity" (blue vertical shaded area), "intermediate activity" (green oblique shaded area) and "quiescent" (red horizontal shaded area) galaxies. The blue short-dashed lines, the green dotted lines and the red long-dashed lines are the MFs measured at $z = 0.2 - 0.4$ for the "high activity", "intermediate activity" and "quiescent" galaxies, respectively.

Peng, Y.J., Lilly, S., Kovac, K. et al. 2010, ApJ, 721, 193
Sanders, D.B., Salvato, M., Aussel, H. et al. 2007, ApJS, 172, 86
Scoville, N. et al. 2007, ApJS, 172, 1
Springel, V., Frenk, C. S., & White, S. D. M. 2006, Nature, 440, 1137
White, S.D.M. & Rees, M.J. 1978, MNRAS, 183, 341
Williams, R.J., Quadri, R., F., Franx, M. et al., 2009, ApJ, 691, 1879